

Detection of cosmic superstrings by geodesic test particle motion

Betti Hartmann ^{(a),*} Claus Lämmerzahl ^{(b),(c),†} and Parinya Sirimachan ^{(a),‡}

(a) School of Engineering and Science, Jacobs University Bremen, 28759 Bremen, Germany

(b) ZARM, Universität Bremen, Am Fallturm, 28359 Bremen, Germany

(c) Institut für Physik, Universität Oldenburg, 26111 Oldenburg, Germany

(Dated: February 16, 2022)

(p,q)-strings are bound states of p F-strings and q D-strings and are predicted to form at the end of brane inflation. As such these cosmic superstrings should be detectable in the universe. In this paper we argue that they can be detected by the way that massive and massless test particles move in the space-time of these cosmic superstrings, in particular we study solutions to the geodesic equation in the space-time of field theoretical (p,q)-strings. The geodesics can be classified according to the test particle's energy, angular momentum and momentum in the direction of the string axis. We discuss how the change of the magnetic fluxes, the ratio between the symmetry breaking scale and the Planck mass, the Higgs to gauge boson mass ratios and the binding between the F- and D-strings, respectively, influence the motion of the test particles. While massless test particles can only move on escape orbits, a new feature as compared to the infinitely thin string limit is the existence of bound orbits for massive test particles. In particular, we observe that - in contrast to the space-time of a single Abelian-Higgs string - bound orbits for massive test particles in (p,q)-string space-times are possible if the Higgs boson mass is larger than the gauge boson mass. We also compute the effect of the binding between the p- and the q-string on observables such as the light deflection and the perihelion shift. While light deflection can also be caused by other matter distributions, the possibility of a negative perihelion shift seems to be a feature of finite width cosmic strings that could lead to the unmistakable identification of such objects. In Melvin space-times, which are asymptotically non-conical, massive test particles have to move on bound orbits, while massless test particles can only escape to infinity if their angular momentum vanishes.

PACS numbers: 11.27.+d, 98.80.Cq, 04.40.Nr

* b.hartmann@jacobs-university.de

† laemmerzahl@zarm.uni-bremen.de

‡ p.sirimachan@jacobs-university.de

I. INTRODUCTION

Cosmic strings are topological defects that are predicted to have formed via the Kibble mechanism [1] during one of the phase transitions in the early universe and in the field theoretical description [2] can be considered to be an example of a topological soliton. Due to the fact that these objects can be extremely heavy (up to 10^{12} kg/m) they were believed to be a possible source of the density perturbations that led to structure formation and the anisotropies in the cosmic microwave background (CMB) [3]. However, the detailed measurement of the CMB power spectrum as obtained by COBE, BOOMERanG and WMAP showed that cosmic strings cannot be the main source for these anisotropies.

In recent years cosmic strings gained renewed interest due to the possible connection to the fundamental entities of String Theory [4]. Brane inflation is a popular inflationary model that can be embedded into String Theory and predicts the formation of cosmic string networks at the end of inflation [5]. E.g. in the framework of type IIB String Theory the inflaton field corresponds to the distance between two Dirichlet branes with 3 spatial dimensions (D3-branes) and inflation ends when these two branes collide and annihilate. The production of strings (and lower dimensional branes) then results from the collision of these two branes. Each of the original D3-branes has a $U(1)$ gauge symmetry that gets broken when the branes annihilate. If the gauge combination is Higgsed, magnetic flux tubes of this gauge field carrying Ramond-Ramond (R-R) charge are D-branes with one spatial dimension, so-called D-strings. When the gauge combination is confined the field is condensated into electric flux tubes carrying Neveu-Schwarz-Neveu Schwarz (NS-NS) charges and these objects are fundamental strings (F-strings) [6]. D-strings and F-strings are so-called cosmic superstrings [4] which seem to be a generic prediction of supersymmetric hybrid inflation [7] and grand unified based inflationary models [8]. D- and F-strings, however, have different properties than the usual (solitonic) cosmic strings. The probability of intercommutation of solitonic strings is equal to one but less than one in the case of cosmic superstring. Therefore, solitonic strings do not merge, while cosmic superstrings tend to form bound states. When p F-strings and q D-strings interact, they can merge and form bound states, so-called (p,q) -strings [9] whose properties have been investigated [10]. Even though the origin of (p,q) -strings is type IIB string theory, their properties can be investigated in the framework of field theoretical models [11–14]. The influence of gravity on field theoretical (p,q) -strings has been studied in [15].

Since there are good reasons for cosmic superstrings to be a consequence of String Theory it is very exciting to search for observational consequences of their existence. There has been considerable effort in numerically modeling cosmic string networks to obtain CMB power and polarization spectra [16]. Comparison with observations has shown that cosmic strings might well contribute considerably to the energy density of the universe. There is another way to detect cosmic strings in the universe, namely through the motion of test bodies in such string space-times. The test particle motion in different space-times containing cosmic strings has been investigated in [17–21], while the complete set of orbits of test particles in the space-time of black hole pierced by an infinitely thin cosmic string has been given for a Schwarzschild black hole in [22] and for a Kerr black hole in [23].

In this paper we follow the latter approach and use the field theoretical model discussed in [15] to describe (p,q) -strings by two coupled Abelian-Higgs models in curved space-time. For vanishing coupling between the two sectors, the model corresponds to the Abelian-Higgs model coupled minimally to gravity. This model has solutions describing strings with finite core width that have been investigated in [24, 25]. Geodesics in this space-time have been studied recently [26] and can only be given numerically. Here we would like to extend this investigation to the field theoretical description of cosmic superstrings.

Our paper is organized as follows: in Section II, we discuss the field theoretical model that possesses (p,q) -string solutions and we also work out the geodesic equation. In Section III we discuss our numerical results, in particular we give examples of orbits and demonstrate how the ratio between the symmetry breaking scale and the Planck mass, the ratios between Higgs and gauge boson masses, the magnetic fluxes and the binding between the F- and D-string influence our results. We conclude in Section IV.

II. THE MODEL

A. The space-time of a (p,q) -string

The field theoretical model to describe gravitating (p,q) -strings reads [15]

$$S = \int d^4x \sqrt{-g} \left(\frac{1}{16\pi G} R + \mathcal{L}_m \right), \quad (1)$$

where R is the Ricci scalar and G is Newton's constant. The matter Lagrangian \mathcal{L}_m is given by [11]

$$\mathcal{L}_m = D_\mu \phi (D^\mu \phi)^* - \frac{1}{4} F_{\mu\nu} F^{\mu\nu} + D_\mu \xi (D^\mu \xi)^* - \frac{1}{4} H_{\mu\nu} H^{\mu\nu} - u(\phi, \xi) \quad (2)$$

with the covariant derivatives $D_\mu \phi = \nabla_\mu \phi - ie_1 A_\mu \phi$, $D_\mu \xi = \nabla_\mu \xi - ie_2 B_\mu \xi$ of the two complex scalar fields (Higgs fields) ϕ and ξ and the field strength tensors $F_{\mu\nu} = \nabla_\mu A_\nu - \nabla_\nu A_\mu = \partial_\mu A_\nu - \partial_\nu A_\mu$, $H_{\mu\nu} = \nabla_\mu B_\nu - \nabla_\nu B_\mu = \partial_\mu B_\nu - \partial_\nu B_\mu$ of two U(1) gauge potential A_μ , B_ν with coupling constants e_1 and e_2 . ∇_μ denotes the gravitational covariant derivative. Finally, the potential $V(\phi, \xi)$ reads:

$$u(\phi, \xi) = \frac{\lambda_1}{4} (\phi\phi^* - \eta_1^2)^2 + \frac{\lambda_2}{4} (\xi\xi^* - \eta_2^2)^2 - \lambda_3 (\phi\phi^* - \eta_1^2)(\xi\xi^* - \eta_2^2), \quad (3)$$

where λ_1 and λ_2 are the self-couplings of the two scalar fields, while $\lambda_3 > 0$ is the coupling between the two sectors. η_1 and η_2 are the vacuum expectation values of the scalar fields.

In order for both U(1) symmetries to spontaneously break which then leads to the formation of strings we have to require that the (absolute) minimum of the potential (3) is at non-vanishing values of $|\phi|$ and $|\xi|$. This leads to the requirement [11]

$$\lambda_1 \lambda_2 > 4\lambda_3^2. \quad (4)$$

The most general static cylindrically symmetric line element invariant under boosts along the z -direction is

$$ds^2 = N(\rho)^2 dt^2 - d\rho^2 - L(\rho)^2 d\varphi^2 - N(\rho)^2 dz^2. \quad (5)$$

For the matter and gauge fields, we apply the Ansatz [2]

$$\phi(\rho, \varphi) = \eta_1 h(\rho) e^{in\varphi}, \quad A_\mu dx^\mu = \frac{1}{e_1} (n - P(\rho)) d\varphi \quad (6)$$

$$\xi(\rho, \varphi) = \eta_2 f(\rho) e^{im\varphi}, \quad B_\mu dx^\mu = \frac{1}{e_2} (m - R(\rho)) d\varphi, \quad (7)$$

where n and m are integers indexing the vorticity of the two Higgs fields around the z -axis and correspond to the degree of the map from $S^1 \rightarrow S^1$, where the homotopy group is $\pi_1(S^1) = \mathbb{Z}$. In our field theoretical model of (p,q)-strings the p corresponds to the winding n and the q to the winding m .

We can then do the following rescaling

$$\rho \rightarrow \frac{\rho}{e_1 \eta_1}, \quad L \rightarrow \frac{L}{e_1 \eta_1} \quad (8)$$

such that the total Lagrangian only depends on the following dimensionless coupling constants

$$\gamma = 8\pi G \eta_1^2, \quad g = \frac{e_2}{e_1}, \quad q = \frac{\eta_2}{\eta_1}, \quad \beta_i = \frac{\lambda_i}{e_i^2}, \quad (9)$$

where $i = 1, 2, 3$. γ is proportional to the ratio between the Planck mass $M_{\text{Pl}} = G^{-1/2}$ and the symmetry breaking scale η_1 . Moreover, $\sqrt{\beta_1}$ is proportional to the ratio between the Higgs mass $M_{\text{H},1} = \sqrt{\lambda_1} \eta_1$ and the corresponding gauge boson mass $M_{\text{W},1} = \sqrt{2} e_1 \eta_1$, while $\sqrt{\beta_2}/g$ is proportional to the ratio between the Higgs mass $M_{\text{H},2} = \sqrt{\lambda_2} \eta_2$ and the corresponding gauge boson mass $M_{\text{W},2} = \sqrt{2} e_2 \eta_2$. Each of the strings possesses a scalar core with width $\rho_{\text{H},i} \sim M_{\text{H},i}^{-1}$ and a gauge field core with width $\rho_{\text{W},i} \sim M_{\text{W},i}^{-1}$, $i = 1, 2$. Note that with the rescaling (8) the width of the gauge field cores is $\rho_{\text{W},1} \sim 1/\sqrt{2}$, $\rho_{\text{W},2} \sim 1/(gq\sqrt{2})$ while the widths of the scalar cores is given by $\rho_{\text{H},i} = 1/\sqrt{\beta_i}$, $i = 1, 2$.

The variation of the action (1) with respect to the matter fields leads to the following equations [15]

$$\frac{(N^2 L h')'}{N^2 L} = \frac{P^2 h}{L^2} + \frac{1}{2} \frac{\partial u}{\partial h}, \quad (10)$$

$$\frac{(N^2 L f')'}{N^2 L} = \frac{R^2 f}{L^2} + \frac{1}{2} \frac{\partial u}{\partial f}, \quad (11)$$

$$\frac{L}{N^2} \left(\frac{N^2 P'}{L} \right)' = 2h^2 P, \quad (12)$$

$$\frac{L}{N^2} \left(\frac{N^2 R'}{L} \right)' = 2g^2 f^2 R, \quad (13)$$

where the prime denotes the derivative with respect to ρ and the potential u reads

$$u(h, f) = \frac{\beta_1}{4}(h^2 - 1)^2 + \frac{\beta_2}{4}(f^2 - q^2)^2 - \beta_3(h^2 - 1)(f^2 - q^2) . \quad (14)$$

The variation of (1) with respect to the metric leads to the Einstein equations

$$R_{\mu\nu} = -\gamma \left(T_{\mu\nu} - \frac{1}{2} g_{\mu\nu} T \right) , \quad (15)$$

where T is the trace of the energy momentum tensor. Using our Ansatz these read [15]

$$\frac{(LNN')'}{N^2L} = \gamma \left[\frac{(P')^2}{2L^2} + \frac{(R')^2}{2g^2L^2} - u \right] , \quad (16)$$

$$\frac{(N^2L')'}{N^2L} = -\gamma \left[\frac{2h^2P^2}{L^2} + \frac{2R^2f^2}{L^2} + \frac{(P')^2}{2L^2} + \frac{(R')^2}{2g^2L^2} + u \right] . \quad (17)$$

In addition there is a constraint equation that is not independent. This reads

$$2 \frac{N'L'}{NL} + \frac{(N')^2}{N^2} = \gamma \left[(h')^2 + (f')^2 + \frac{(P')^2}{2L^2} + \frac{(R')^2}{2g^2L^2} - \frac{h^2P^2}{L^2} - \frac{R^2f^2}{L^2} - u \right] . \quad (18)$$

The set of differential equations can be solved only numerically subject to an appropriate set of boundary conditions. The requirement of regularity at $\rho = 0$ leads to the following conditions

$$h(0) = 0, \quad f(0) = 0, \quad P(0) = n, \quad R(0) = m \quad (19)$$

for the matter fields and

$$N(0) = 1, \quad N'(0) = 0, \quad L(0) = 0, \quad L'(0) = 1 \quad (20)$$

for the metric fields, while the requirement of finiteness of the energy per unit length leads to

$$h(\infty) = 1, \quad f(\infty) = q, \quad P(\infty) = 0, \quad R(\infty) = 0 . \quad (21)$$

The inertial energy per unit length $E_{\text{in}}^{(n,m)}$ of the (p,q)-string is given by

$$E_{\text{in}}^{(n,m)} = \int \sqrt{-g_3} T_0^0 d\rho d\varphi \quad (22)$$

$$= 2\pi \int_0^\infty NL \left((h')^2 + (f')^2 + \frac{(P')^2}{2L^2} + \frac{(R')^2}{2g^2L^2} + \frac{h^2P^2}{L^2} + \frac{R^2f^2}{L^2} + u \right) d\rho , \quad (23)$$

where g_3 is the determinant of the 2+1-dimensional space-time given by (t, ρ, φ) . Note that there is also another notion of energy in this space-time, namely that of the Tolman energy [24, 25]. This defines the gravitationally active mass.

In the Bogomolnyi-Prasad-Sommerfield (BPS) limit [27] given by $\beta_1 = \beta_2 \equiv \beta = 2$, $\beta_3 = 0$ and with the choice $q = g = 1$ we have that $T_\rho^\rho = T_\varphi^\varphi = 0$ such that it follows from (16) that $N(\rho) \equiv 1$. The remaining BPS equations are

$$h' = \frac{Ph}{L} , \quad f' = \frac{Rf}{L} , \quad (24)$$

$$\frac{P'}{L} = h^2 - 1 , \quad \frac{R'}{L} = f^2 - 1 , \quad (25)$$

for the matter fields and

$$\frac{L''}{L} = -\gamma \left[\frac{2h^2P^2}{L^2} + \frac{2R^2f^2}{L^2} + (h^2 - 1)^2 + (f^2 - 1)^2 \right] \quad (26)$$

for the non-trivial metric function. The solutions fulfill an energy bound such that

$$E_{\text{in}}^{(n,m)} = 2\pi(n + m) . \quad (27)$$

Note that in this limit the widths of the scalar cores $\rho_{H,i}$ become equal to the widths of the respective gauge field cores $\rho_{W,i}$, $i = 1, 2$.

The binding energy per unit length of a (p,q)-string $E_b^{(n,m)}$ can be defined as

$$E_b^{(n,m)} = E_{\text{in}}^{(n,m)} - nE_{\text{in}}^{(n,0)} - mE_{\text{in}}^{(0,m)} . \quad (28)$$

Finally the (p,q)-string possesses magnetic fields in z -direction $\vec{B}_1 = B_1 \vec{e}_z$ and $\vec{B}_2 = B_2 \vec{e}_z$ with

$$B_1 = -\frac{P'}{L} , \quad B_2 = -\frac{R'}{L} , \quad (29)$$

where B_1 and B_2 are given in units of $M_{W,1}^2$. The magnetic fluxes then read

$$\Phi_{M,1} = 2\pi n , \quad \Phi_{M,2} = 2\pi m \quad (30)$$

and are obviously quantized. Hence, changing the winding numbers n and m changes the magnetic fluxes along the (p,q)-string.

B. The geodesic equation

The Lagrangian \mathcal{L}_g describing geodesic motion of a test particle in the static cylindrically symmetric space-time (5) reads

$$\mathcal{L}_g = g_{\mu\nu} \frac{dx^\mu}{d\tau} \frac{dx^\nu}{d\tau} = \varepsilon = N^2 \left(\frac{dt}{d\tau} \right)^2 - \left(\frac{d\rho}{d\tau} \right)^2 - L^2 \left(\frac{d\varphi}{d\tau} \right)^2 - N^2 \left(\frac{dz}{d\tau} \right)^2 , \quad (31)$$

where $\varepsilon = 0, 1$ for massless or massive test particles, respectively and τ is an affine parameter that corresponds to the proper time for massive test particles moving on time-like geodesics. The space-time has three Killing vectors $\frac{\partial}{\partial t}$, $\frac{\partial}{\partial \varphi}$ and $\frac{\partial}{\partial z}$ which lead to the following constants of motion: the energy E , the angular momentum L_z along the string axis (z -axis) and the momentum p_z

$$N^2 \frac{dt}{d\tau} =: E , \quad L^2 \frac{d\varphi}{d\tau} =: L_z , \quad N^2 \frac{dz}{d\tau} =: p_z . \quad (32)$$

Using the rescaling (8) the constants of motion must be rescaled according to $E \rightarrow E/(e_1 \eta_1)$, $p_z \rightarrow p_z/(e_1 \eta_1)$, $L_z \rightarrow L_z/(e_1 \eta_1)^2$. We then find from (31)

$$\varepsilon = N^2 \left(\frac{dt}{d\tau} \right)^2 - \left(\frac{d\rho}{d\tau} \right)^2 - L^2 \left(\frac{d\varphi}{d\tau} \right)^2 - N^2 \left(\frac{dz}{d\tau} \right)^2 = \frac{E^2 - p_z^2}{N^2} - \left(\frac{d\rho}{d\tau} \right)^2 - \frac{L_z^2}{L^2} . \quad (33)$$

Using the constants of motion we find from (31)

$$\frac{1}{2} \left(\frac{d\rho}{d\tau} \right)^2 = \frac{E^2 - \varepsilon}{2} - \frac{1}{2} \left[E^2 \left(1 - \frac{1}{N^2} \right) + \frac{p_z^2}{N^2} + \frac{L_z^2}{L^2} \right] . \quad (34)$$

The left hand side of (34) is always positive and $E^2 - \varepsilon$ is a constant of motion. Following [28] we can then rewrite this equation as

$$\frac{1}{2} \left(\frac{d\rho}{d\tau} \right)^2 = \mathcal{E} - V_{\text{eff}}(\rho) , \quad (35)$$

where

$$V_{\text{eff}}(\rho) = \frac{1}{2} \left[E^2 \left(1 - \frac{1}{N^2} \right) + \frac{p_z^2}{N^2} + \frac{L_z^2}{L^2} \right] \quad (36)$$

is the effective potential and $\mathcal{E} = (E^2 - \varepsilon)/2$. Note that with this definition the effective potential becomes explicitly energy-dependent.

In the following, we would like to find $t(\rho)$, $\varphi(\rho)$ and $z(\rho)$. For this, we rewrite the geodesic equation in the form

$$d\varphi = \pm \frac{L_z d\rho}{L(\rho)^2 \left(\frac{E^2 - p_z^2}{N(\rho)^2} - \frac{L_z^2}{L(\rho)^2} - \varepsilon \right)^{1/2}}, \quad (37)$$

$$dz = \pm \frac{p_z d\rho}{N(\rho)^2 \left(\frac{E^2 - p_z^2}{N(\rho)^2} - \frac{L_z^2}{L(\rho)^2} - \varepsilon \right)^{1/2}}, \quad (38)$$

$$dt = \pm \frac{E d\rho}{N(\rho)^2 \left(\frac{E^2 - p_z^2}{N(\rho)^2} - \frac{L_z^2}{L(\rho)^2} - \varepsilon \right)^{1/2}}. \quad (39)$$

The solution for each component can then be calculated as a function of ρ by using numerical integration methods.

III. NUMERICAL RESULTS

We have solved the set of differential equations (10) - (17) numerically using the ODE solver COLSYS that uses a Newton-Raphson adaptive grid method [29]. The relative error of the solutions is on the order of 10^{-13} - 10^{-10} . Each component of the geodesic equation can then be integrated numerically by using the integrating function `quad`, i.e. a recursive adaptive Simpson quadrature in MATLAB with an absolute error tolerance 10^{-8} . However the numerical profiles of the metric functions $N(\rho)$ and $L(\rho)$ must first be interpolated. This was done using a piecewise cubic Hermite interpolating polynomial, i.e. with `pchip` in MATLAB. With this procedure it is possible to obtain a smooth curve for the effective potential.

In the following we will distinguish between bound orbits, escape orbits and terminating orbits. Note that when we talk about bound, escape and terminating orbits we are referring to the motion in the x - y -plane. The particles can, of course, move along the full z -axis from $-\infty$ to $+\infty$ for $p_z \neq 0$.

Bound orbits are orbits on which test particles move from a minimal value of ρ , $\rho_{\min} > 0$ to a maximal value of ρ , $\rho_{\max} < \infty$ and back again. These orbits have hence two turning points with $(d\rho/d\tau)^2 = 0$. On escape orbits, on the other hand, particles come from $\rho = \infty$, reach a minimal value of ρ , $\rho_{\min} > 0$ and move back to $\rho = \infty$, which means that escape orbits have only one turning point with $(d\rho/d\tau)^2 = 0$. Looking at (35) it is obvious that turning points are located at those ρ at which $\mathcal{E} - V_{\text{eff}}(\rho) = 0$. Finally, terminating orbits are orbits that end at the string axis $\rho = 0$.

For all our calculations we have chosen $q = 1$ and $g = 1$.

A. Generalities

Solutions to the model (1) have been extensively studied previously. The Table I summarizes the particular cases.

Solution	β_1, β_2	β_3	γ	Studied in
Abelian-Higgs string in flat space-time	$\beta_1 = \beta_2 \neq 0$	$\beta_3 = 0$	$\gamma = 0$	[2]
Abelian-Higgs string in curved space-time	$\beta_1 = \beta_2 \neq 0$	$\beta_3 = 0$	$\gamma \neq 0$	[24], [25]
(p,q)-string in flat space-time	$\beta_1 = \beta_2 = 2$	$\beta_3 \neq 0$	$\gamma = 0$	[11]
(p,q)-string in curved space-time	$\beta_1 = \beta_2 = 2$	$\beta_3 \neq 0$	$\gamma \neq 0$	[15]

TABLE I. Known string solutions of the model (1).

It has been observed in [24] that there are two types of solutions if one couples the Abelian-Higgs model minimally to gravity: string solutions and Melvin solutions which exist for the same values of the parameters in the model. These differ by their asymptotic behaviour of the metric functions at infinity.

1. String solutions

The string solution behaves like

$$N(\rho \rightarrow \infty) = c_1, \quad L(\rho \rightarrow \infty) = c_2 \rho + c_3, \quad c_2 > 0, \quad (40)$$

where c_1 , c_2 and c_3 are constants depending on n , m , g , γ and β_i , $i = 1, 2, 3$. For $\beta_3 = 0$ it has been found [24, 25] that $c_1 > 1$ for $\beta_1 = \beta_2 \equiv \beta < 2$, $c_1 < 1$ for $\beta_1 = \beta_2 \equiv \beta > 2$ and $c_1 = 1$ in the BPS limit $\beta_1 = \beta_2 \equiv \beta = 2$.

A solution with the asymptotics (40) describes a conical space-time with deficit angle δ given by

$$\delta = 2\pi(1 - c_2) \quad (41)$$

In linear order the deficit angle δ is given by the product of the coupling γ and the inertial energy per unit length $E_{\text{in}}^{(n+m)}$ with $\delta \sim \gamma E_{\text{in}}^{(n+m)}$. As such the constant $c_2 = 1$ for $\gamma = 0$ (or $E_{\text{in}}^{(n+m)} = 0$) and c_2 decreases for either γ or $E_{\text{in}}^{(n+m)}$ increasing. If the coupling γ or the energy per unit length is too large then $c_2 < 0$ and the deficit angle $\delta > 2\pi$. In this case the solution would have a singularity at a finite, parameter-dependent value of $\rho = \rho_0$ with $L(\rho = \rho_0) = 0$, while $N(\rho_0)$ stays finite. These solutions are the so-called super-massive string solutions [30] (or inverted string solutions). We will not consider these kind of solutions in this paper and will always assume the deficit angle to be smaller than 2π .

The “force” exerted on a test particle corresponds to the right hand side of

$$\frac{d^2\rho}{d\tau^2} = - \left(\frac{E^2 - p_z^2}{N^3} \right) N' + \left(\frac{L_z^2}{L^3} \right) L' . \quad (42)$$

Note that for string solutions the effective potential tends asymptotically to a constant with $V_{\text{eff}}(\rho \rightarrow \infty) \rightarrow \frac{E^2(c_1^2 - 1) + p_z^2}{2c_1^2}$ and hence there is no force exerted on test particles far from the string. While the force associated to the angular momentum L_z is always repulsive, the total force close to the string can either be attractive or repulsive. Since $E^2 - p_z^2 \geq 0$ and $N > 0$ this depends on the sign of N' (see more details below).

For $\rho \ll 1$ the string solutions behave like

$$N(\rho \ll 1) \sim 1 + O(\rho^2) , \quad L(\rho \ll 1) \sim \rho . \quad (43)$$

Hence there is an infinite potential barrier at $\rho = 0$ for test particles with non-vanishing angular momentum L_z , i.e. these test particles can never reach the string axis at $\rho = 0$ since there is no force to counterbalance the repulsive centrifugal force. On the other hand, for $L_z = 0$ the effective potential tends to a constant $V_{\text{eff}}(\rho \rightarrow 0) \rightarrow p_z^2/2$. Hence particles with $E^2 - \varepsilon < p_z^2$ can reach the string axis. Since $E^2 > p_z^2$ these terminating orbits are only possible for massive test particles with $\varepsilon = 1$.

Infinitely thin cosmic strings The infinitely thin limit corresponds to the case where both the width of the scalar core as well as that of the gauge field core tend to zero. The string is hence a 1-dimensional object that can e.g. be described by the Nambu-Goto action. In this case the metric function $N(\rho) \equiv 1$ (or some other constant that can be absorbed into the definition of t) and $L(\rho) \equiv c_2\rho$ for $\rho > 0$. In this case, the only component in the force (42) exerted on a particle is the repulsive angular momentum contribution. Hence, bound orbits are not possible in this space-time. This can also easily be understood when noting that the space-time of an infinitely thin cosmic string is locally flat [3] and geodesics are just straight lines. The fact that bound orbits are possible in a finite width cosmic string space-time is related to the fact that close to the string axis the conical space-time is smoothed on scales comparable to the width of the string. The existence of bound orbits in “pure” cosmic string space-times [31] is hence a new feature when considering cosmic strings with finite width.

2. Melvin solutions

The Melvin solutions exist for the same parameter values as the string solutions, but have a different asymptotic behaviour:

$$N(\rho \rightarrow \infty) \rightarrow a_1\rho^{2/3} , \quad L(\rho \rightarrow \infty) \rightarrow a_2\rho^{-1/3} , \quad (44)$$

where again a_1 and a_2 are parameter dependent positive constants. This space-time is not asymptotically flat and the proper length of a curve with $t = \text{const.}$, $\rho = \text{const.}$, $z = \text{const}$ and $\varphi = 0 \rightarrow 2\pi$ is $s = 2\pi a_2\rho^{-1/3}$. This tends to zero for $\rho \rightarrow \infty$. For the Melvin space-time with the asymptotic behaviour (44) the effective potential tends to infinity asymptotically with $V_{\text{eff}}(\rho \rightarrow \infty) \propto \rho^{2/3}$ for $L_z \neq 0$. Hence there is an infinite potential barrier at infinity for test particles with non-vanishing angular momentum, i.e. these particles can never reach infinity. This is related to the fact that the total force (42) on a test particle is always attractive at large ρ in Melvin space-times. For $L_z = 0$, the effective potential tends to $E^2/2$ for $\rho \rightarrow \infty$. Hence, the asymptotic value of the effective potential is always larger than (for massive test particles) or equal to (for massless test particles) \mathcal{E} . Massive test particles moving on radial geodesics can thus not reach infinity, while massless test particles have a turning point at infinity.

For $\rho \ll 1$ the Melvin solutions behave like the string solutions (43).

B. Geodesic motion in (p,q)-string space-times: string solutions

We will mainly discuss the geodesic motion in space-times with the asymptotic behaviour (40) since we believe this to be the physically relevant case. However, since the Melvin solution is a solution to the Abelian-Higgs model coupled minimally to gravity, we will also comment on this below.

1. The effective potential

The case $\beta_3 = 0$, $\beta_1 = \beta_2 \equiv \beta$ has been discussed for $n = m = 1$ in [26]. It was found that bound orbits are only possible for $\beta < 2$ and for massive particles. In fact, in order to have bound orbits we need (at least) two turning points of the motion, i.e. two intersection points between V_{eff} and \mathcal{E} . Note that for \mathcal{E} finite and larger than the minimal value of the effective potential we will always have one intersection point for $L_z \neq 0$ due to the infinite potential barrier at small ρ such that escape orbits always exist. However, bound orbits are only possible if in addition the effective potential has local minima and maxima with $\frac{dV_{\text{eff}}}{d\rho} = 0$. At these local extrema we should then have

$$\frac{E^2 - p_z^2}{L_z^2} = \frac{N(\rho)^3}{N'(\rho)} \frac{L'(\rho)}{L(\rho)^3}. \quad (45)$$

Since $E^2 - p_z^2 > 0$, $N(\rho) > 0$, $L(\rho) > 0$, $L'(\rho) > 0$ this equation has only solutions for $N'(\rho) > 0$. For $\beta_3 = 0$ it has been observed [26] that the metric function $N(\rho)$ is either monotonically decreasing (for $\beta > 2$) or monotonically increasing (for $\beta < 2$), while $N(\rho) \equiv 1$ in the BPS limit $\beta = 2$. Hence the sign of $N'(\rho)$ doesn't change and in particular, bound orbits are only possible for $\beta < 2$. In this case the energy-momentum part of the force (42) becomes attractive for $\beta < 2$, i.e. if the width of the scalar core is larger than the width of the gauge field core and can balance the repulsive part associated to the angular momentum. On the other hand for $\beta = 2$ ($\beta > 2$) the width of the scalar core is equal (smaller) than the width of the gauge field core. We observe that this leads to a vanishing (repulsive) energy-momentum part in the force (42) and only escape orbits are possible.

This is different when $\beta_3 > 0$. We will first discuss the case $n = m = 1$. The behaviour of the metric function $N(\rho)$ of a (1,1)-string for $\gamma = 0.3$ and different choices of β_i , $i = 1, 2, 3$ is shown in Fig. 1. In all cases the blue dotted-dashed line corresponds to $\beta_3 = 0$ and for cases (a), (b) and (c) the green solid line corresponds to $\beta_3 \approx \beta_3^{(\text{max})}$ with $\beta_3^{(\text{max})} \equiv \sqrt{\beta_1 \beta_2}/2$ the maximally allowed value for a given choice of β_1 and β_2 . For (a) $\beta_1 = 1$, $\beta_2 = 2$, (b) $\beta_1 = \beta_2 = 2$ and (c) $\beta_1 = \beta_2 = 1$ the increase of β_3 leads to an increase of the asymptotic value of $N(\rho)$ for all choices of the β_i , $i = 1, 2, 3$. Hence, the increased binding between the p- and the q-string pronounces the effect already observed in the $\beta_3 = 0$ limit. Note that while bound orbits are not possible in the BPS limit $\beta_1 = \beta_2 = 2$ for $\beta_3 = 0$ bound orbits do exist for $\beta_3 > 0$ and $\beta_1 = \beta_2 = 2$ (which, of course, no longer corresponds to a BPS limit). For (d) $\beta_1 = 1.5$, $\beta_2 = 6$, (e) $\beta_1 = 2$, $\beta_2 = 4.5$ and (f) $\beta_1 = 2.25$, $\beta_2 = 4$ the metric function $N(\rho)$ can have a local minimum if $\beta_3 < \beta_3^{(\text{cr})}(\beta_1, \beta_2)$, i.e. if the binding between the strings is not too large. This is new as compared to the $\beta_3 = 0$ limit. We find that $\beta_3^{(\text{cr})}(1.5, 6) \approx 0.7$, $\beta_3^{(\text{cr})}(2, 4.5) \approx 0.66$, $\beta_3^{(\text{cr})}(2.25, 4) \approx 0.51$.

Obviously, for (a) $\beta_1 < 2$, $\beta_2 = 2$, (b) $\beta_1 = \beta_2 = 2$ and (c) $\beta_1 < 2$, $\beta_2 < 2$ the metric function $N(\rho)$ increases monotonically, while for the other cases $N(\rho)$ can first decrease from $N(\rho = 0) = 1$, have a local minimum at $\rho = \rho_{\text{min}}$ with $N(\rho_{\text{min}}) < 1$ and then increase again to $N(\rho \gg 1) > 1$. This has important consequences for the shape of the effective potential as discussed below and can be understood as follows: consider the (1,1)-string to be a superposition of a (1,0)-string and a (0,1)-string. Now, for $\beta_3 = 0$, these two strings do not interact. In this case, we know that for $\beta_i > 2$, $i = 1, 2$ the metric function $N(\rho)$ would monotonically decrease, while for $\beta_j < 2$, $j = 1, 2$ the metric function $N(\rho)$ would monotonically increase. Superposing a string with $\beta_i > 2$ and one with $\beta_j < 2$ leads then to a metric function $N(\rho)$ that first decreases and then increase again. Note that the opposite is not possible since the scalar core of a string with $\beta_i > 2$ is smaller than that of a string with $\beta_j < 2$.

This behaviour of the metric function $N(\rho)$ leads to the observation that the effective potential can have a negative minimum which for $p_z = 0$ is located exactly at ρ_{min} . In the case $\beta_3 = 0$, the effective potential can have a local minimum for $\beta < 2$, but this will always be positive valued since $N'(\rho) > 0$ means $N(\rho) > 1$. This is shown in Fig.2 for a particle with $E = 0.01$, $L_z = 0.03$ and $p_z = 0$. For cases (a), (b) and (c) the effective potential is positive for all values of ρ for non-vanishing L_z or p_z , while it can become negative for the other cases. In fact, the potential becomes positive everywhere for $\beta_3 \approx \beta_3^{(\text{cr})}$. This will have influence on the existence of bound orbits as discussed below. In particular if the potential has a negative valued minimum as is e.g. the case for $\beta_1 = 1.5$, $\beta_2 = 6$ and $\beta_3 = 0.7$, particles with $\mathcal{E} < 0$, i.e. $E^2 < 1$ can move on bound orbits.

We have also investigated how the metric function $N(\rho)$ changes when changing the winding numbers n , m and hence the magnetic fluxes along the string. Our results are shown in Fig.3 for $\gamma = 0.3$.

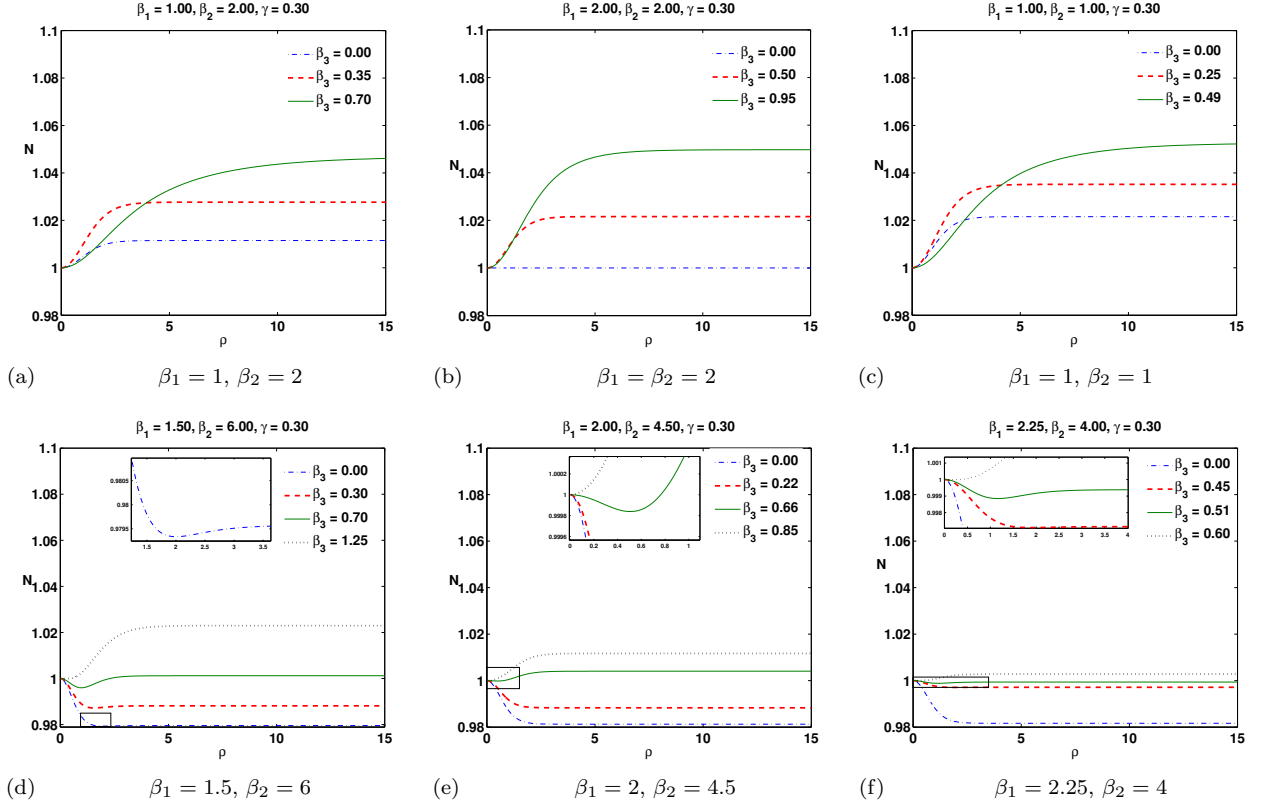


FIG. 1. The metric function $N(\rho)$ of a (1,1)-string is shown for $\gamma = 0.3$ and different choices of β_1 , β_2 and β_3 .

We observe that the increase in the total magnetic flux along the string increases the asymptotic value of the metric function $N(\rho)$ if $N'(\rho) > 0$. The qualitative features do not change. If a minimum of the metric function exists for $n = m = 1$ it exists for all choices of n and m (see Fig.3(d)) and if $N'(\rho) > 0$ for $n = m = 1$ this will be the same for other choices of n and m .

Note that the profiles of the metric functions $L(\rho)$ for all cases are similar to those for $\beta_3 = 0$. The deviation of $L'(\rho \gg 1) = c_2$ from one determines the deficit angle of the space-time and depends on the inertial mass per unit length. This is shown for $\gamma = 0.3$ and different choices of n , m and β_i in Fig.4. For solutions with $\beta_1 = \beta_2$ the slope of $L(\rho)$ at infinity decreases with increasing sum $n + m \equiv p + q$. This is natural since an increase in the windings leads to an increase in the mass per unit length and hence to an increase of the deficit angle. Moreover, for a given sum $p + q$ the solutions with $p = q$ have the biggest slope of $L(\rho)$ at infinity. This is related to the fact that the solutions with equal winding are bound strongest (see also the results in [15]).

2. Classification of solutions

The geodesics can be classified according to the test particles energy E , angular momentum L_z and momentum in the direction of the string axis p_z . Intersection points of \mathcal{E} with the effective potential, i.e. points where $\mathcal{E} = V_{\text{eff}}$ correspond to turning points of the motion. The maximum and minimum of the effective potential determine the largest, respectively smallest possible value of \mathcal{E} for bound orbits. The effective potential is determined by the metric functions N and L as well as the constants of motion. Choosing β_i , $i = 1, 2, 3$, γ and n , m we find the numerical profiles of N and L . For a given L_z^2 (and $\varepsilon = 0$ or $\varepsilon = 1$) there is an E^2 such that the value of \mathcal{E} is equal to the maximal value of the effective potential $V_{\text{eff}}(\rho)$ and one E^2 such that \mathcal{E} is equal to the minimal value of $V_{\text{eff}}(\rho)$. In the former case, the corresponding orbit is an unstable circular orbit, while in the latter the orbit is a stable circular orbit.

Defining $\mu := E^2$ and $\nu := L_z^2$ we can then plot the domain of existence of bound orbits in the μ - ν -plane. Our results for massive particles with $p_z = 0$ are given in Figs 5, 6 for $n = m = 1$. Fig.5 corresponds to the case of a (p,q)-string space-time with monotonically increasing $N(\rho)$ and Fig. 6 to the case of a (p,q)-string space-time which

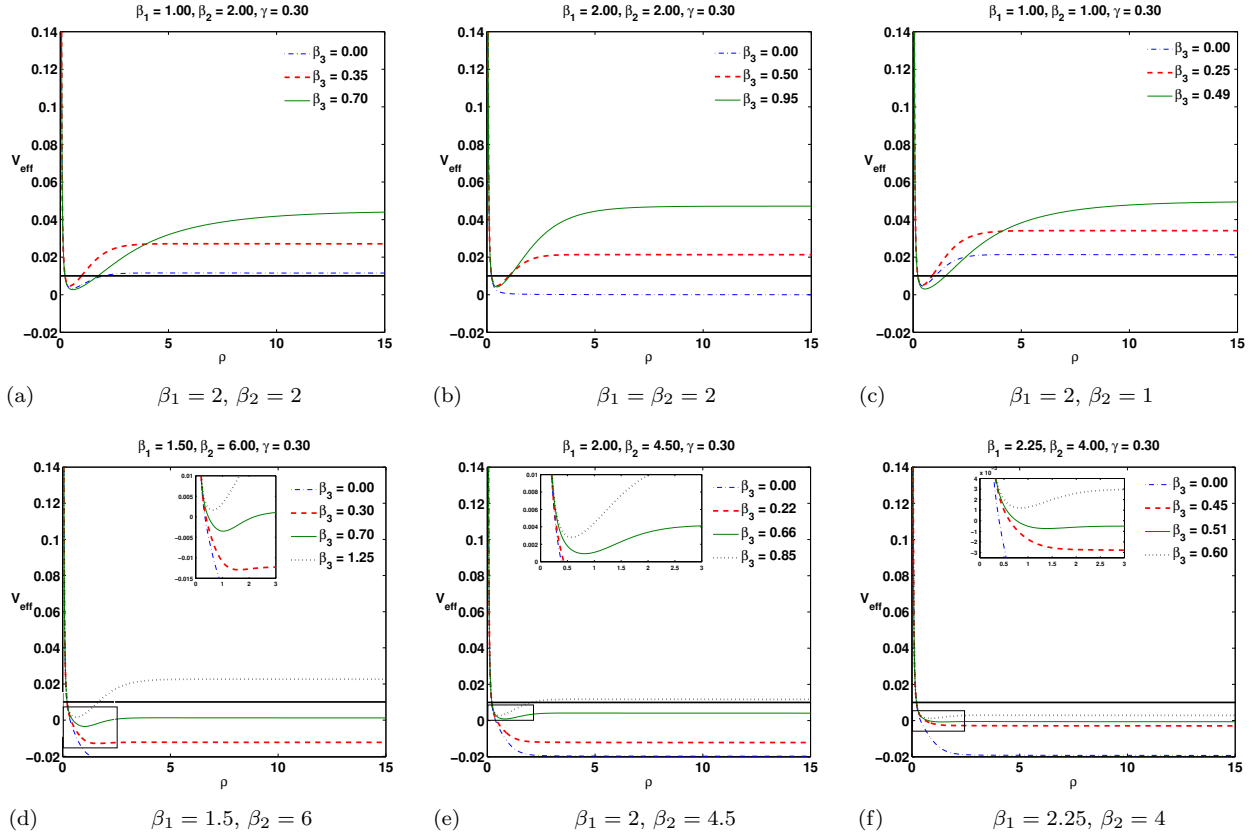


FIG. 2. The effective potential $V_{\text{eff}}(\rho)$ in the space-time of a (1,1)-string is shown for $\gamma = 0.3$ and different choices of β_1 , β_2 and β_3 . Here $E = 0.01$, $L_z = 0.03$ and $p_z = 0$.

has $N'(\rho) = 0$ at some non-vanishing, finite value of ρ . The blue dashed and solid black line from $(\mu_1, 0)$ to (μ_3, ν_3) and $(\mu_2, 0)$ to (μ_3, ν_3) , respectively, represent the choice of (E, L_z, p_z) for stable and unstable circular orbits, respectively, and bound orbits exist in the colored domain between the two bounding curves. (μ_3, ν_3) corresponds to the largest possible values of μ and ν for bound orbits. M1 denotes the domain in the μ - ν -plane in which \mathcal{E} is smaller than the minimum of the effective potential and hence there are no solutions to the geodesic equation. M4 denotes the domain in which \mathcal{E} is larger than the maximum of the effective potential and only escape orbits are possible. In M2 and M3 on the other hand bound orbits are possible. In M2 \mathcal{E} is smaller than the asymptotic value of the effective potential, but larger than the minimum of V_{eff} and only bound orbits are possible. In M3 \mathcal{E} is larger than the asymptotic value of the effective potential but smaller than the maximum of V_{eff} . Hence, in M3 there are bound orbits, but escape orbits are also possible.

For $\beta_1 = \beta_2 = 2$ and $\beta_3 > 0$ we find that $\mu_1 = 1$ for all values of β_3 , while μ_2 as well as (μ_3, ν_3) increase with increasing β_3 . While for $\beta_1 = \beta_2 = 2$, $\beta_3 = 0$ no bound orbits exist at all [26], bound orbits are possible for $\beta_3 = 0.1$ and the domain of existence of bound orbits in the μ - ν -plane is extending for increasing β_3 (compare the plots for $\beta_3 = 0.1$ and $\beta_3 = 0.75$). The existence of bound orbits in the limit where $M_{H,i} = M_{W,i}$, $i = 1, 2$ is new as compared to the $\beta_3 = 0$ case.

This, however, is not the only difference as compared to the space-time of an Abelian-Higgs string. As stated above we find that it is possible to have negative valued minima of the effective potential in (p,q)-string space-times. This leads to the observation that massive test particles with $\mu < 1$ can now move on bound orbits. This is a new feature as compared to the $\beta_3 = 0$ case, where we had to require that $\mu > 1$. This means that test particles with less energy can move on bound orbits in (p,q)-string space-times as compared to the $\beta_3 = 0$ case, which corresponds to the space-time of two non-interacting Abelian-Higgs strings. This is clearly seen in Fig. 6 for $\gamma = 0.35$, $\beta_1 = 10$, $\beta_2 = 3.6$ and two different values of β_3 . While for $M_{H,i} > M_{W,i}$, $i = 1, 2$ and in the $\beta_3 = 0$ limit no bound orbits exist [26] they exist in a small domain of the μ - ν -plane for sufficiently large β_3 . The extension of the domain in the μ - ν -plane for which bound orbits exist increases with increasing β_3 , i.e. the values of μ_1 , μ_2 and (μ_3, ν_3) increase.

The change of the μ - ν -plot of a (p,q)-string with $\gamma = 0.2$, $\beta_1 = 8$, $\beta_2 = 0.5$, $\beta_3 = 0.99$ resulting from the change

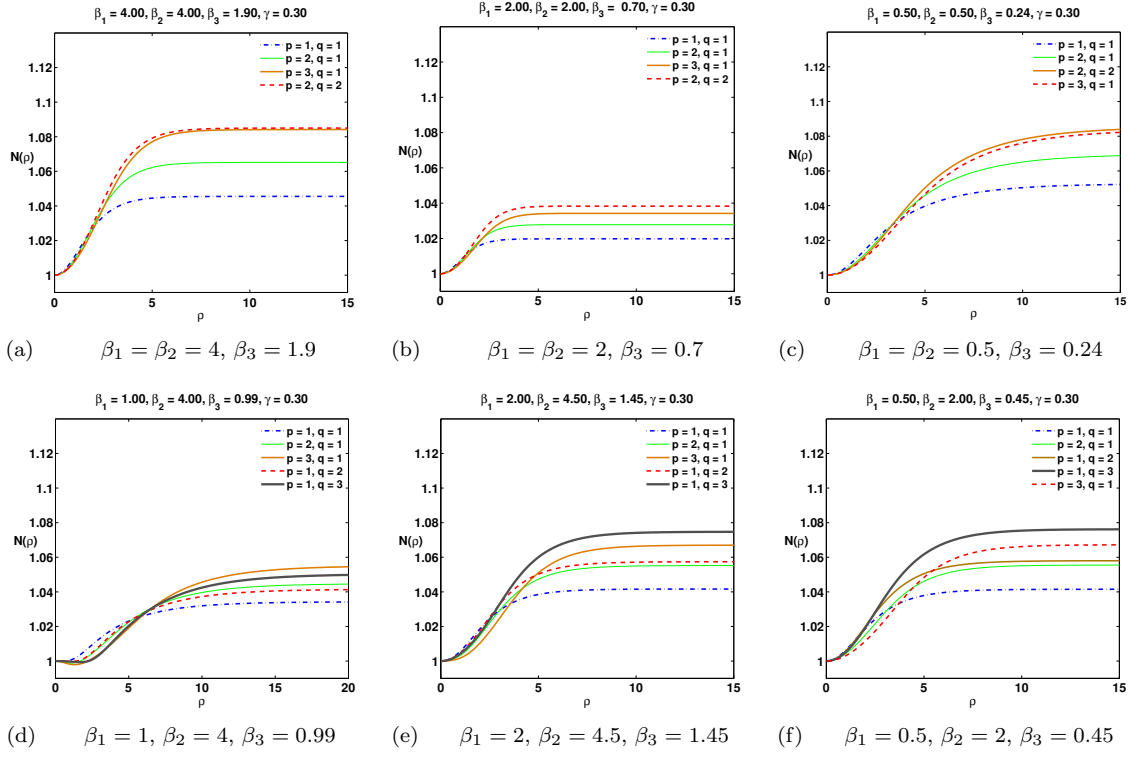


FIG. 3. The metric function $N(\rho)$ of a (p,q) -string for $\gamma = 0.3$, different choices of β_i , $i = 1, 2, 3$ and different choices of $(p,q) \equiv (n, m)$.

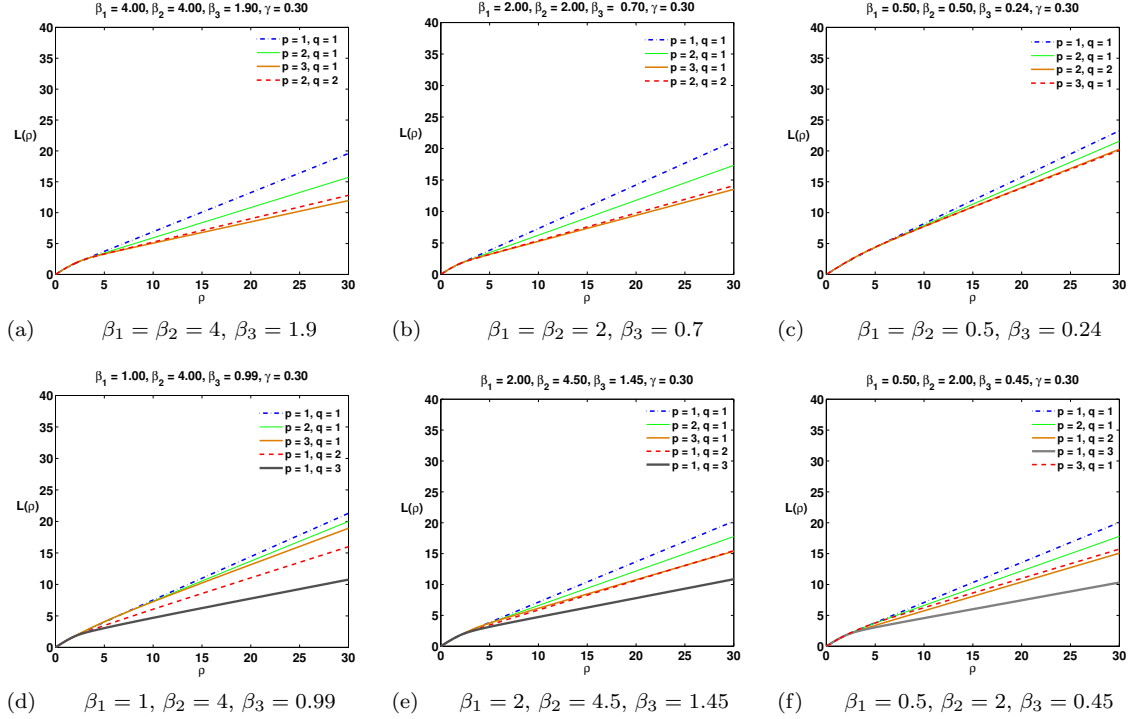


FIG. 4. The metric function $L(\rho)$ of a (p,q) -string for $\gamma = 0.3$, different choices of β_i , $i = 1, 2, 3$ and different choices of $(p,q) \equiv (n, m)$.

of the winding numbers $(p,q) \equiv (n,m)$ and hence the change of the magnetic fluxes along the (p,q) -string are shown in Fig.7. Here we concentrate on the case of a string with $\rho_{H,1} < \rho_{W,1}$ (the p-string) interacting with a string that has $\rho_{H,2} > \rho_{W,2}$ (the q-string). Increasing the winding of the p-string while keeping the winding of the q-string fixed shifts μ_1 and μ_2 to lower values, while the difference $\mu_2 - \mu_1$ slightly increases with increasing p . Hence bound orbits are possible in a slightly bigger domain of the μ - ν -plane and in particular test particles need less energy to be able to move on bound orbits when increasing the winding of the p-string. On the other hand, increasing the winding of the q-string while keeping the winding of the p-string fixed increases the value of μ_2 , while μ_1 is nearly constant. Again, the domain of existence of bound orbits becomes larger when increasing the winding of the q-string.

For $p_z \neq 0$, the qualitative features are the same. We observe, however, that the whole domain of existence of bound orbits shifts to larger values of μ when increasing p_z . This is obviously related to the fact the effective potential V_{eff} is energy-dependent (see (36)).

In contrast to massive test particles, we find that massless particles can only move on escape orbits. This is very similar to what has been observed in the $\beta_3 = 0$ limit [26] and agrees with the result found in [32] which states that for a general cosmic string space-time with topology $\mathbb{R}^2 \times \Sigma$ massless test particles must move on geodesics that escape to infinity in both directions, i.e. closed geodesics are not possible. The assumption made in [32] is that Σ must have positive Gaussian curvature. To show that Σ has positive Gaussian curvature in our case, we rewrite the metric (5) for massless particles ($ds^2 = 0$) moving in a plane parallel to the x - y -plane as follows

$$dt^2 = \frac{1}{N^2} d\rho^2 + \frac{L^2}{N^2} d\varphi^2 = \tilde{g}_{ij} dx^i dx^j \quad , \quad i = 1, 2 \quad (46)$$

where \tilde{g}_{ij} is the so-called optical metric [33] of which the spatial projection of geodesics of massless particles, i.e. light rays are geodesics. \tilde{g}_{ij} is the metric of the above mentioned 2-manifold Σ and has Gaussian curvature K given by

$$K = \frac{L'}{L} N' N - \frac{L''}{L} N^2 - (N')^2 + N N'' \quad . \quad (47)$$

For $\beta_1 = \beta_2 = 2$ and $\beta_3 = 0$ (the BPS limit) we know that $N \equiv 1$ and the Gaussian curvature is obviously positive, away from the BPS limit one has to use the numerical solution and compute the curvature. We find that for most values of β_1 , β_2 , β_3 and γ the Gaussian curvature is indeed positive and our result is in agreement with that of [32]. However, if β_1 and β_2 are sufficiently large and β_3 sufficiently small, we find that K can become negative close to the string axis. Though the theorem of [32] is not applicable here, we nevertheless find that bound orbits do not exist.

3. Examples of orbits

In Fig.8 we show how a massive test particle with $E = 0.995$, $L_z = 0.022$ and $p_z = 0.011$ moves around a $(1,1)$ -string with $\gamma = 0.35$, $\beta_1 = 10$, $\beta_2 = 3.6$ and different choices of β_3 . Note that the orbit is not planar due to the fact that the test particle has momentum in z -direction (see (38)). The red and blue circles indicate the width of the scalar cores and the gauge field cores, while the dotted circles denote the minimal and maximal radius of the orbit. For our choice of parameters the width of the gauge field cores is larger than that of the scalar cores. We observe that the larger β_3 the closer the test particle moves around the string. For $\beta_3 = 2.1$, the orbit extends out to roughly four times the radius of the gauge field core, while for $\beta_3 = 2.2$ the maximal radius is only roughly twice that of the gauge field core. Stating it differently: for smaller β_3 the test particle moves mainly in the exterior vacuum region of the string, while for larger β_3 it moves mainly close to or inside the string core, where the matter fields are non-trivial. As stated above, bound orbits are only possible in a limited domain of the μ - ν -plane. Test particles with values of E and L_z outside of this domain will not be able to move on a bound orbit around the string and will escape to infinity. An example of such an escape orbit of a massive test particle is shown in Fig.9. Since the radii of the scalar and gauge field cores are very small in comparison to the extension of the orbit, we denote the core by a blue dot. The blue dashed line indicates the minimal radius of the orbit. We observe that the test particle comes from infinity, encircles the string core once and then moves again away to infinity for $\beta_3 = 2.15$ and $\beta_3 = 2.48$. For $\beta_3 = 2.96$ the particle gets simply deflected by the string without encircling it. In fact, the deflection is decreasing for increasing β_3 . This can be explained by the fact that the energy per unit length and hence the deficit angle decreases with increasing β_3 .

We have also studied how the orbits change when changing the winding numbers $(p,q) = (n,m)$ and hence the magnetic fluxes. This is shown in Fig. 10 for the bound orbit of a massive test particle with $E = 0.9931$, $L_z = 0.01$ and $p_z = 0.015$ in the space-time of a (p,q) -string with $\gamma = 0.2$, $\beta_1 = 8$, $\beta_2 = 0.5$, $\beta_3 = 0.99$. While for $(p,q) = (1,1)$ and $(p,q) = (1,2)$ the test particle moves close to the core of the string, it can extend considerably into the vacuum region for $(p,q) = (2,1)$. Apparently, the change of the winding of the q-string which has $\rho_{H,2} > \rho_{W,2}$ mainly influences the perihelion shift of the orbit, which increases with increasing winding. On the other hand the increase of the winding of the p-string which has $\rho_{W,1} > \rho_{H,1}$ allows the test particle to move further away from the string core.

The change of an escape orbit of a massless test particle with the change of the windings is shown in Fig.11. While for $(p,q) = (1,1)$ and $(p,q) = (1,3)$ the test particle gets simply deflected by the string it encircles the string before escaping to infinity for $(p,q) = (3,1)$. Apparently, the change of the winding of the q-string which has $\rho_{H,2} > \rho_{W,2}$ influences the deflection only slightly. On the other hand the increase of the winding of the p-string which has $\rho_{W,1} > \rho_{H,2}$ leads to an encirclement of the string.

C. Geodesic motion in Melvin space-times

In Fig.12 we show the effective potential for a Melvin space-time with $\beta_1 = \beta_2 = 0.4$, $\beta_3 = 0.18$ and $\gamma = 0.57$ and test particle parameters $E = 10$, $p_z = 5$, $L_z = 1.1$. In comparison, we also give the effective potential of the corresponding string space-time. Close to the z -axis the effective potential of the Melvin space-time is equivalent to that of a string space-time. In contrast to the string space-time the effective potential in a Melvin space-time will always have a local minimum (see also (45)) and $V_{\text{eff}}(\rho \rightarrow \infty) \rightarrow \infty$ for $L_z \neq 0$. Hence there will be only bound orbits, while escape orbits do not exist. As already mentioned this is related to the fact that the space-time is not asymptotically flat and particles can never reach infinity. This is interesting since in string space-times a massless test particle will always escape from the string, while a massive test particle can move on a bound orbit provided both energy E and angular momentum L_z are not too large. In Melvin space-times test particles will always move on bound orbits. In Fig. 13 we show the bound orbit for a massless test particle with $E = 10$, $L_z = 1.1$, $p_z = 5$ moving in a Melvin space-time with $\beta_1 = \beta_2 = 0.4$, $\beta_3 = 0.18$, $\gamma = 0.57$.

IV. OBSERVABLES

Since we believe the string space-time to be the physically relevant case, we compute all observables in the space-time with asymptotic behaviour (40).

A. Perihelion shift

The perihelion shift of a bound orbit of a massive test particle ($\varepsilon = 1$) can be calculated by the following expression

$$\delta\varphi_{\varepsilon=1} = 2 \int_{\rho_{\min}}^{\rho_{\max}} \frac{L_z d\rho}{L(\rho)^2 \left(\frac{E^2 - p_z^2}{N(\rho)^2} - \frac{L_z^2}{L(\rho)^2} - 1 \right)^{1/2}} - 2\pi, \quad (48)$$

where ρ_{\min} and ρ_{\max} are the minimal and the maximal radius of the bound orbit, respectively. The dependence of the perihelion shift $\delta\varphi_{\varepsilon=1}$ of a bound planar orbit of a massive test particle with $E = 1.01$, $L_z = 0.02$, $p_z = 0$ on the binding parameter β_3 is shown in Fig.14(a). For this particular case, the perihelion shift is negative which means that the test particle moves from the minimal to the maximal radius and returns back to the minimal radius under an angle less than 2π . In asymptotically flat black hole space-times and even asymptotically flat space-times of black holes pierced by infinitely thin cosmic strings (see [22, 23]) the perihelion shift is positive. In a Schwarzschild-(Anti)-de Sitter black hole space-time the positive (negative) cosmological constant gives a positive (negative) contribution to the perihelion shift. Since all observations point to a positive cosmological constant, we would expect that the perihelion shift is positive for astrophysically relevant black hole solutions. Note that in the space-time of an infinitely thin cosmic string alone no bound orbits exist (see discussion above) and hence it makes no sense to calculate the perihelion shift. On the other hand, the presence of an infinitely thin cosmic string in black hole space-times enhances the (positive) perihelion shift [22]. The fact that the perihelion shift can become negative in the case of finite width cosmic strings is hence related to the fact that the space-time is that of a smoothed cone close to the string axis. In fact, the absolute value of the perihelion shift increases with increasing β_3 , i.e. for increasing β_3 the change of the φ coordinate from the first to the second minimal radius decreases. This can be understood when considering the influence of β_3 on the effective potential. In fact, the potential becomes steeper when increasing β_3 and hence the difference between the minimal and the maximal radius for fixed values of E , L_z and p_z decreases. Moreover, we observe that the perihelion shift for a (p,q) -string with $M_{H,i} > M_{W,i}$, $i = 1, 2$ has the largest negative value, while a (p,q) -string with $M_{H,i} < M_{W,i}$, $i = 1, 2$ has the smallest negative value.

We have also studied whether the perihelion shift is always negative and find that it becomes positive for cosmic string space-times with coupling constants chosen such that the deficit angle is close to 2π and the values of E and L_z are large, i.e. close to the boundary of the μ - ν -domain in which bound orbits exist (see Figs 5-7). In this case, the difference between ρ_{\min} and ρ_{\max} is quite large and the test particle shows mainly in the vacuum region outside the

string. We find e.g. for a p-q-string space-time with $\beta_1 = \beta_2 = 4$, $\beta_3 = 1.02$, $\gamma = 0.499963$ and resulting deficit angle $\delta/(2\pi) \approx 0.9943$ that the perihelion shift of a bound orbit of a massive test particle with $E = 1.0018$, $L_z = 0.007$ and $p_z = 0$ is positive and has value $\delta\varphi_{\varepsilon=1} \approx 2.3695$ rad.

B. Light deflection

Is it very important for gravitational lensing to understand how massless test particles move on escape orbits.

The deflection of light (massless test particle, i.e. $\varepsilon = 0$) by a (p,q) string can be calculated by the following equation

$$\delta\varphi_{\varepsilon=0} = \int_{\rho_{\min}}^{\infty} \frac{L_z d\rho}{L(\rho)^2 \left(\frac{E^2 - p_z^2}{N(\rho)^2} - \frac{L_z^2}{L(\rho)^2} \right)^{1/2}} - \pi \quad (49)$$

where ρ_{\min} is the minimal radius of the escape orbit of the massless test particle.

The dependence of the deflection $\delta\varphi_{\varepsilon=0}$ of a planar escape orbit of a massless test particle with $E = 1.04$, $L_z = 0.28$, $p_z = 0$ on β_3 is shown in Fig.14(b). The light deflection decreases when increasing β_3 . This is not surprising since the energy per unit length of the (p,q)-string and with it the deficit angle decrease with increasing β_3 .

Moreover, we observe that the light deflection for a (p,q)-string with $M_{H,i} > M_{W,i}$, $i = 1, 2$ has the smallest value, while a (p,q)-string with $M_{H,i} < M_{W,i}$, $i = 1, 2$ has the largest value. This is related to the fact that if the scalar (gauge) field cores dominate strings tend to attract (repel) each other, hence lowering (increasing) the total energy per unit length as compared to the BPS limit. This leads to a decrease (increase) of the deficit angle.

V. CONCLUSIONS

In this paper we have studied test particle motion in the space-time of a cosmic superstring that consists of p D-strings and q F-strings. We have studied the asymptotically conical string space-time as well as the Melvin space-time that has vanishing circumference of a circle at infinity. We observe that the binding between the strings has important effects on the motion of test particles in string space-times. In the $\beta_3 = 0$ limit which corresponds to the space-time of two non-interacting Abelian-Higgs strings and is qualitatively similar to that studied in [26] massive test particles can only move on bound orbits if the scalar core width of the string is larger than that of the gauge field core. For $\beta_3 > 0$ massive test particles can now move on bound orbits if the scalar core width is smaller than the gauge field core width and need less energy than in the $\beta_3 = 0$ limit to do so. The perihelion shift can become negative due to the smoothed conical nature of the space-time close to the string axis and the absolute value of the perihelion shift increases with increasing β_3 . The fact that the perihelion shift can become negative seems to be a characteristic of the space-time of a finite width cosmic string that – to our knowledge – has not been noticed in any other astrophysically relevant space-time yet. Massless particles can only move on escape orbits and the deflection by the string decreases with increasing binding between the p- and the q-string. In Melvin space-times, on the other hand, massless and massive particles cannot escape to infinity and must move on bound orbits.

The deflection of light by cosmic strings should be detectable. Though the identification of cosmic strings due to their gravitational lensing effects has been discussed extensively [34] no such cosmic string lens has been detected to date. Moreover, there might also be other sources of gravitational lensing and when identifying cosmic strings through gravitational lensing it has to be made sure that no “standard” matter distributions are the source of the lensing. On the other hand, the negative perihelion shift seems to be generic to finite width cosmic string space-times. To state it differently: if a negative perihelion shift would be observed this would be a strong evidence for the existence of cosmic strings. The main characteristic of cosmic superstrings is that they can form bound states and our field theoretical solutions describe such bound states. The fact that bound states can form so effectively alters the set of possible orbits considerably in comparison to standard field theoretical cosmic string models. In particular, the mass ratios γ and β_i have an important impact. E.g. the perihelion shift can become positive or negative depending on the choice of these parameters and its absolute value can vary considerably.

Acknowledgments The work of PS was supported by DFG grant HA-4426/5-1.

[1] T. Kibble, J. Phys. A **9** 1378 (1976).

- [2] H. B. Nielsen and P. Olesen, Nucl. Phys. B **61**, 45 (1973).
- [3] A. Vilenkin and P. Shellard, *Cosmic strings and other topological defects*, Cambridge University Press (1994).
- [4] see e.g. J. Polchinski, *Introduction to cosmic F- and D-strings*, hep-th/0412244 and reference therein.
- [5] M. Majumdar and A. C. Davis, JHEP **0203** (2002) 056 [arXiv:hep-th/0202148]. S. Sarangi and S. H. H. Tye, Phys. Lett. B **536**, 185 (2002) [arXiv:hep-th/0204074].
- [6] G. Dvali and A. Vilenkin, JCAP **10** (2004) 03.
- [7] D.H. Lyth and A. Riotto, Phys. Rept. **314** (1999) 1.
- [8] R. Jeannerot, J. Rocher and M. Sakellariadou, Phys. Rev. D **68** (2003) 103514
- [9] E. Copeland, R. Myers and J. Polchinski, JHEP **06** (2004) 013.
- [10] C.J.A.P. Martins, Phys. Rev. **D70**, 107302 (2004); M. Sakellariadou, JCAP **0504** (2005) 003; E.J. Copeland and P.M. Saffin, JHEP **0511**, 023 (2005); S.-H. Tye, I. Wasserman and M. Wyman, Phys. Rev. **D71**, 103508 (2005); M.G. Jackson, N.T. Jones and J. Polchinski, JHEP **10**, 013 (2005); A. Avgoustidis and E.P.S. Shellard, Phys. Rev. D **73** (2006) 041301; M. Hindmarsh and P.M. Saffin, JHEP **0686**, 066 (2006); E.J. Copeland, T.W.B. Kibble, D.A. Steer, Phys. Rev. Lett. **97**, 021602 (2006); E.J. Copeland *et al.*, arXiv:0712.0808 [hep-th]; A. Avgoustidis and E.P.S. Shellard, arXiv: astro-ph/0705.3395; H. Firouzjahi, arXiv:hep-th/0710.4609; R.J. Rivers and D.A. Steer, arXiv:0803.3968 [hep-th]; N. Bevis and P.M. Saffin, arXiv:0804.0200 [hep-th].
- [11] P.M. Saffin, JHEP **0509** (2005) 011.
- [12] A. Rajantie, M. Sakellariadou and H. Stoica, JCAP **11** 021 (2007).
- [13] P.Salmi *et al.*, Phys. Rev. D **77** 041701 (2008).
- [14] J. Urrestilla and A. Vilenkin, JHEP **0802** 037 (2008).
- [15] B. Hartmann and J. Urrestilla, JHEP **07** 006 (2008).
- [16] N. Bevis *et al.*, Phys. Rev. **D75**, 065015 (2007); N. Bevis *et al.*, arXiv:astro-ph/0702223; N. Bevis *et al.*, Phys. Rev. **D76**, 043005 (2007); N. Bevis, M. Hindmarsh, M. Kunz and J. Urrestilla, Phys. Rev. Lett. **100**, 021301 (2008); Phys. Rev. D **75**, 065015 (2007); *for a recent review see* C. Ringeval, *Cosmic strings and their induced non-Gaussianities in the cosmic microwave background*, arxiv: 1005.4842 (astro-ph).
- [17] A. N. Aliev and D. V. Galtsov, Sov. Astron. Lett. **14**, 48 (1988).
- [18] D. V. Galtsov and E. Masar, Class. Quant. Grav. **6**, 1313 (1989).
- [19] S. Chakraborty and L. Biswas, Class. Quant. Grav. **13**, 2153 (1996).
- [20] N. Ozdemir, Class. Quant. Grav. **20** 4409 (2003).
- [21] F. Ozdemir, N. Ozdemir and B. T. Kaynak, Int. J. Mod. Phys. A **19** 1549 (2004).
- [22] E. Hackmann, B. Hartmann, C. Lämmerzahl and P. Sirimachan, Phys. Rev. D **81**, 064016 (2010) [arXiv:0912.2327 [gr-qc]].
- [23] E. Hackmann, B. Hartmann, C. Lämmerzahl and P. Sirimachan, Phys. Rev. D **82**, 044024 (2010) [arXiv:1006.1761 [gr-qc]].
- [24] M. Christensen, A.L. Larsen and Y. Verbin, Phys. Rev. D **60**, 125012 (1999).
- [25] Y. Brihaye and M. Lubo, Phys. Rev. D **62**, 085004 (2000).
- [26] B. Hartmann and P. Sirimachan, JHEP **08** 110 (2010).
- [27] E. B. Bogomolny, Sov. J. Nucl. Phys. **24** (1976) 449 [Yad. Fiz. **24** (1976) 861].
- [28] V. Kagramanova, J. Kunz and C. Lämmerzahl, Gen. Rel. Grav. **40** (2008) 1249.
- [29] U. Ascher, J. Christiansen and R. Russell, Math. of Comp. **33**, 659 (1979); ACM Trans. **7**, 209 (1981).
- [30] D. Garfinkle and P. Laguna, Phys. Rev. D **39**, 1552 (1989); M. E. Ortiz, Phys. Rev. D **43**, 2521 (1991).
- [31] Note that bound orbits exist when combining the space-time of an infinitely thin cosmic string with that of black hole solutions, see e.g. [22, 23].
- [32] G. W. Gibbons, Phys. Lett. B **308**, 237 (1993).
- [33] M. A. Abramowicz, B. Carter and J. P. Lasota, Gen. Rel. Grav. **20**, 1173 (1988).
- [34] M. V. Sazhin *et al.*, Mon. Not. Roy. Astron. Soc. **376** (2007) 1731; M. V. Sazhin, M. Capaccioli, G. Longo, M. Paolillo and O. S. Khovanskaya, arXiv:astro-ph/0601494; Astrophys. J. **636** (2005) L5.

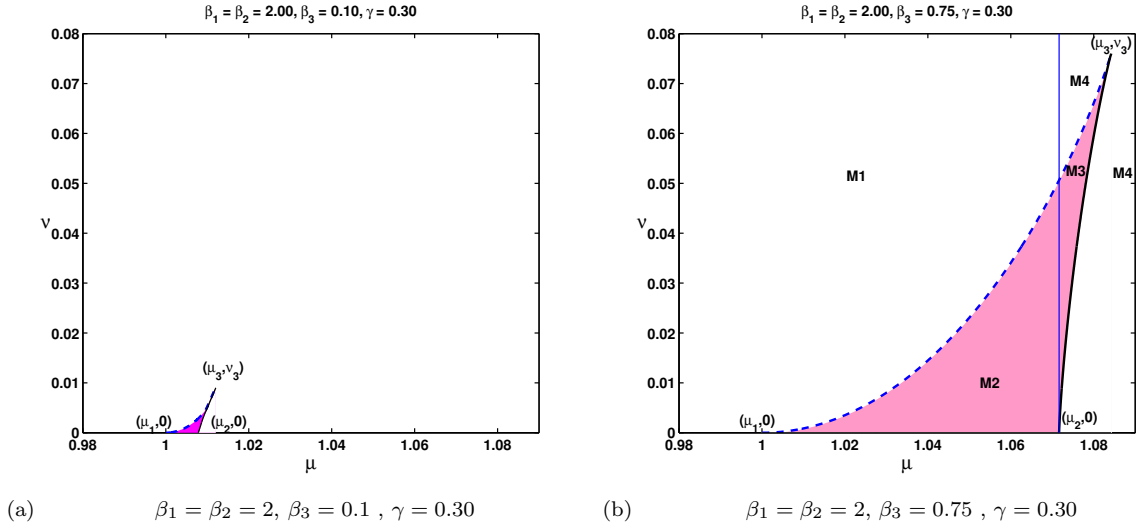


FIG. 5. μ - ν plot for a (1,1)-string space-time with a monotonically increasing $N(\rho)$. Here $\gamma = 0.3$, $\beta_1 = \beta_2 = 2$ and $\beta_3 = 0.1$ (left) and $\beta_3 = 0.75$ (right), respectively. The blue dashed and solid black line represent the choice of (E, L_z, p_z) for stable and unstable circular orbits, respectively. Here $p_z = 0$.

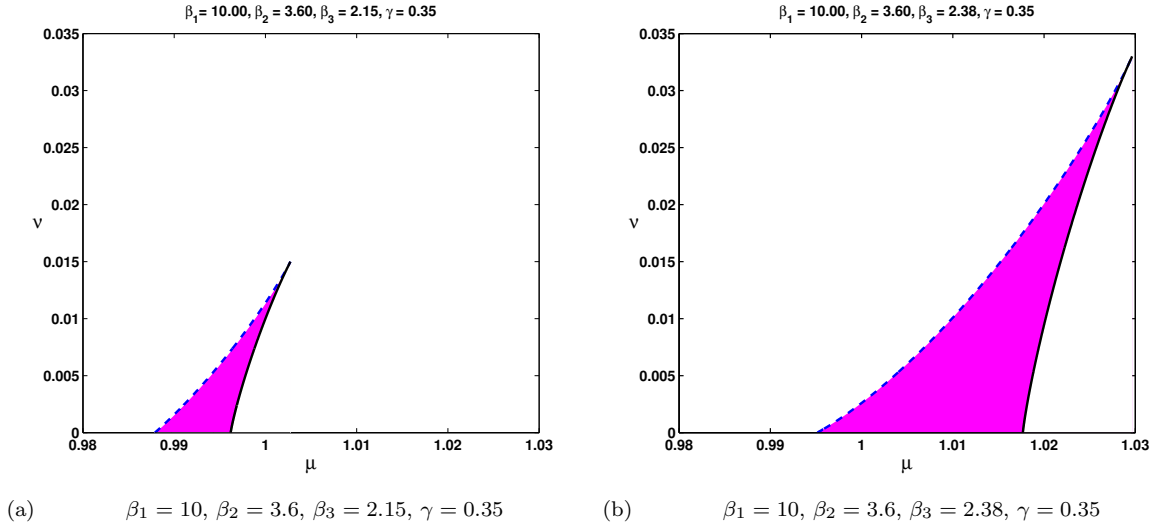


FIG. 6. The μ - ν -plot for a (1,1)-string space-time which has $N'(\rho) = 0$ at some non-vanishing, finite value of ρ . Here $\gamma = 0.35$, $\beta_1 = 10$, $\beta_2 = 3.6$ and two different values of $\beta_3 = 2.15$ (left) and $\beta_3 = 2.38$ (right), respectively. The blue dashed and solid black line represent the choice of (E, L_z, p_z) for stable and unstable circular orbits, respectively. Here $p_z = 0$.

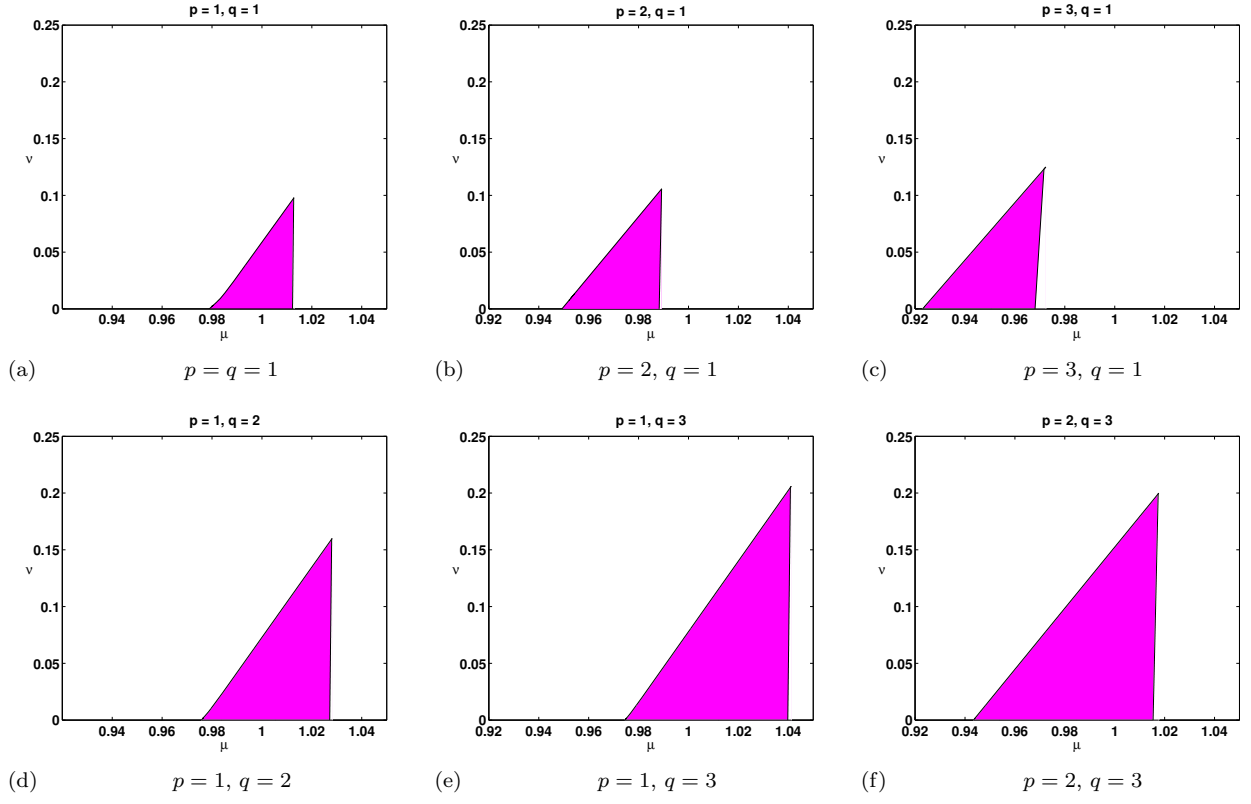


FIG. 7. The μ - ν -plot for a (p,q) -string with $\gamma = 0.2$, $\beta_1 = 8$, $\beta_2 = 0.5$, $\beta_3 = 0.99$ and different choices of $(p,q) \equiv (n,m)$.

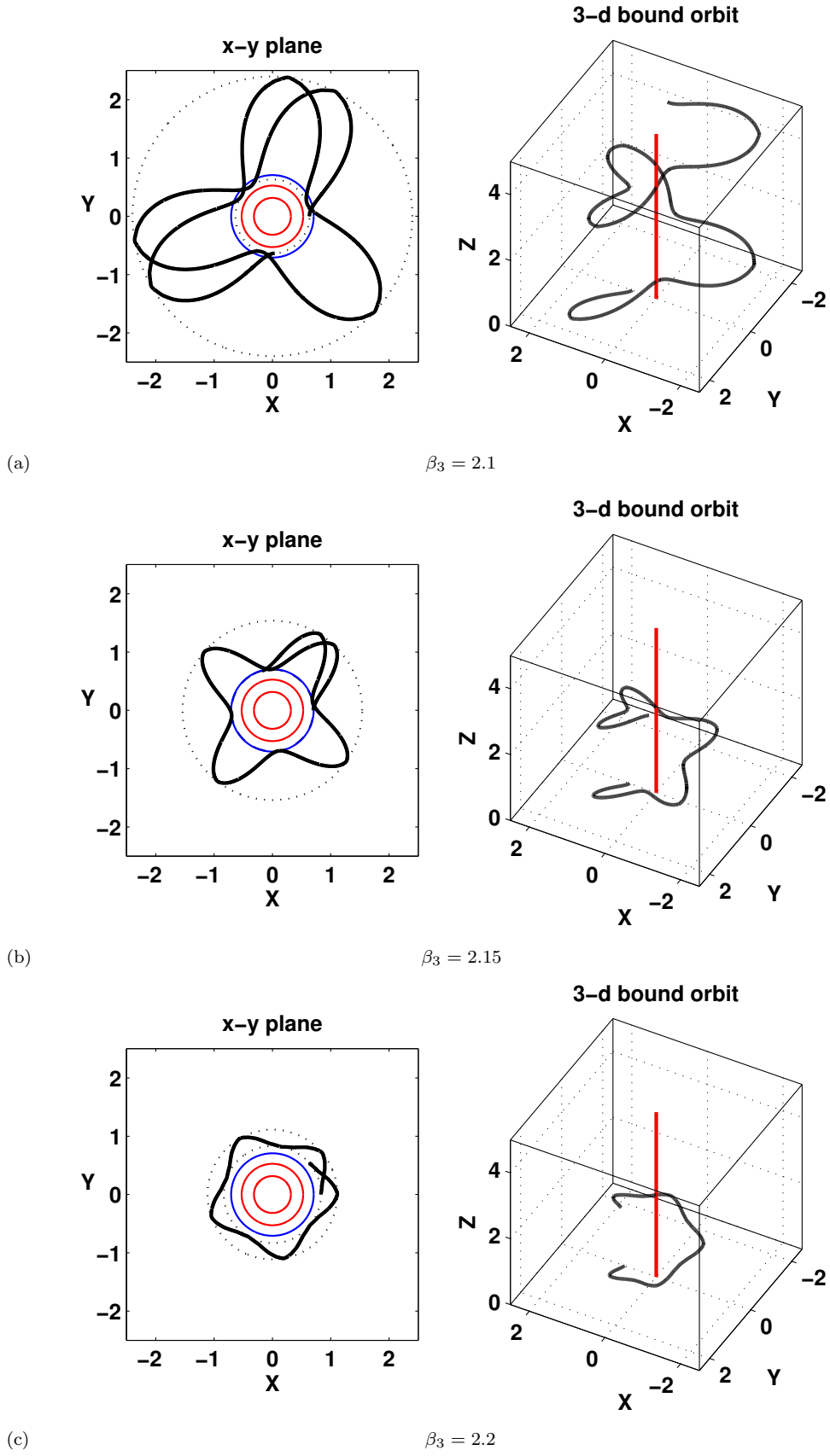


FIG. 8. The bound orbit of a massive test particle with $E = 0.995$, $L_z = 0.022$ and $p_z = 0.011$ in the space-time of a (1,1)-string with $\gamma = 0.3$, $\beta_1 = 10.00$, $\beta_2 = 3.6$ and different choices of β_3 . The dotted circles denote the minimal and the maximal radius of the bound orbit, while the blue and the red circles indicate the radius of the gauge and scalar field cores, respectively.

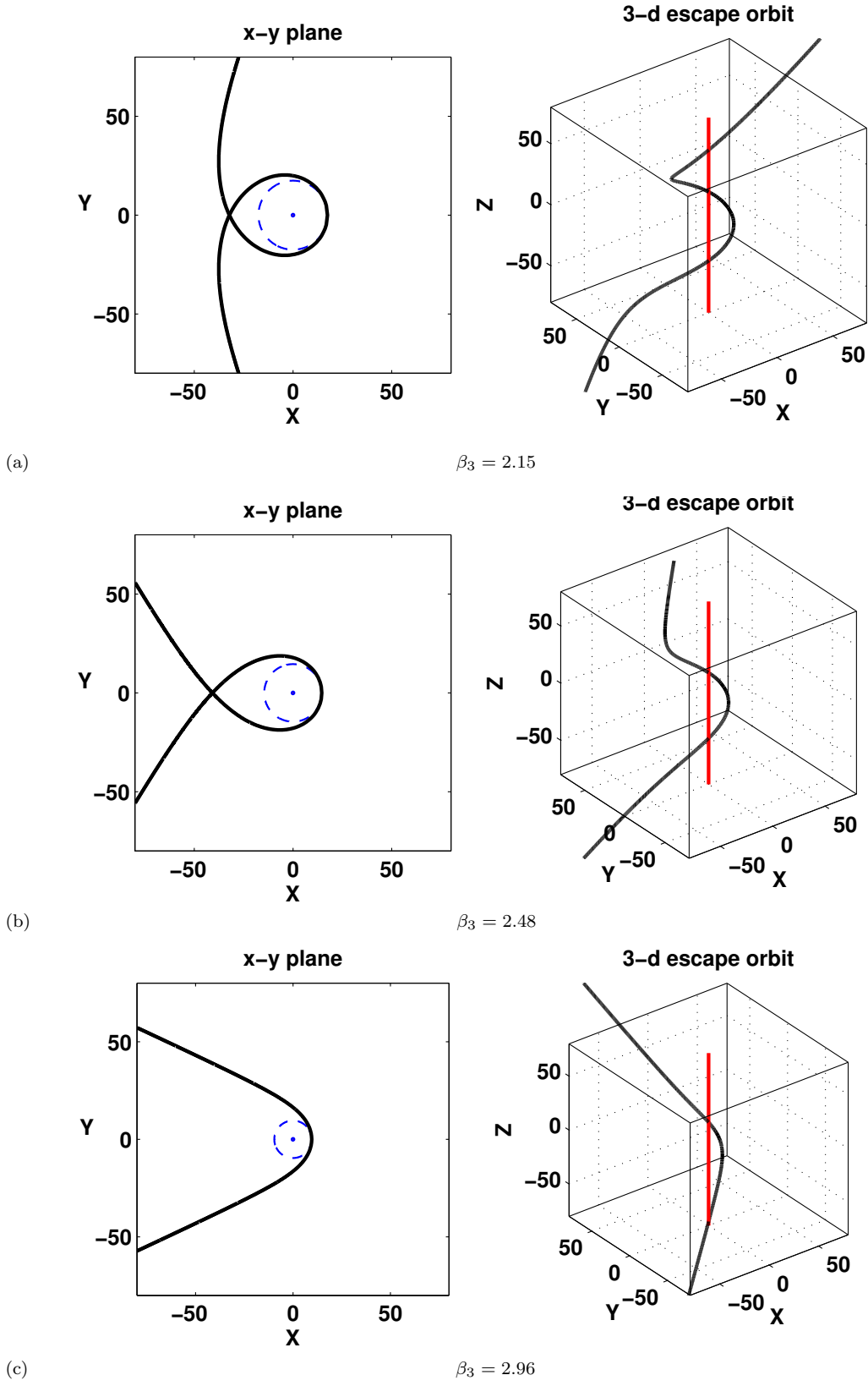


FIG. 9. The escape orbit of a massive test particle with $L_z = 0.02$, $E = 0.06$ and $p_z = 0.05$ in the space-time of a (1,1)-string with $\gamma = 0.35$, $\beta_1 = 10$, $\beta_2 = 3.6$ and different choices of β_3 . The blue dot denotes the core of the string, while the dashed blue line denotes the circle with minimal radius of the orbit, i.e. closest approach of the particle to the string.

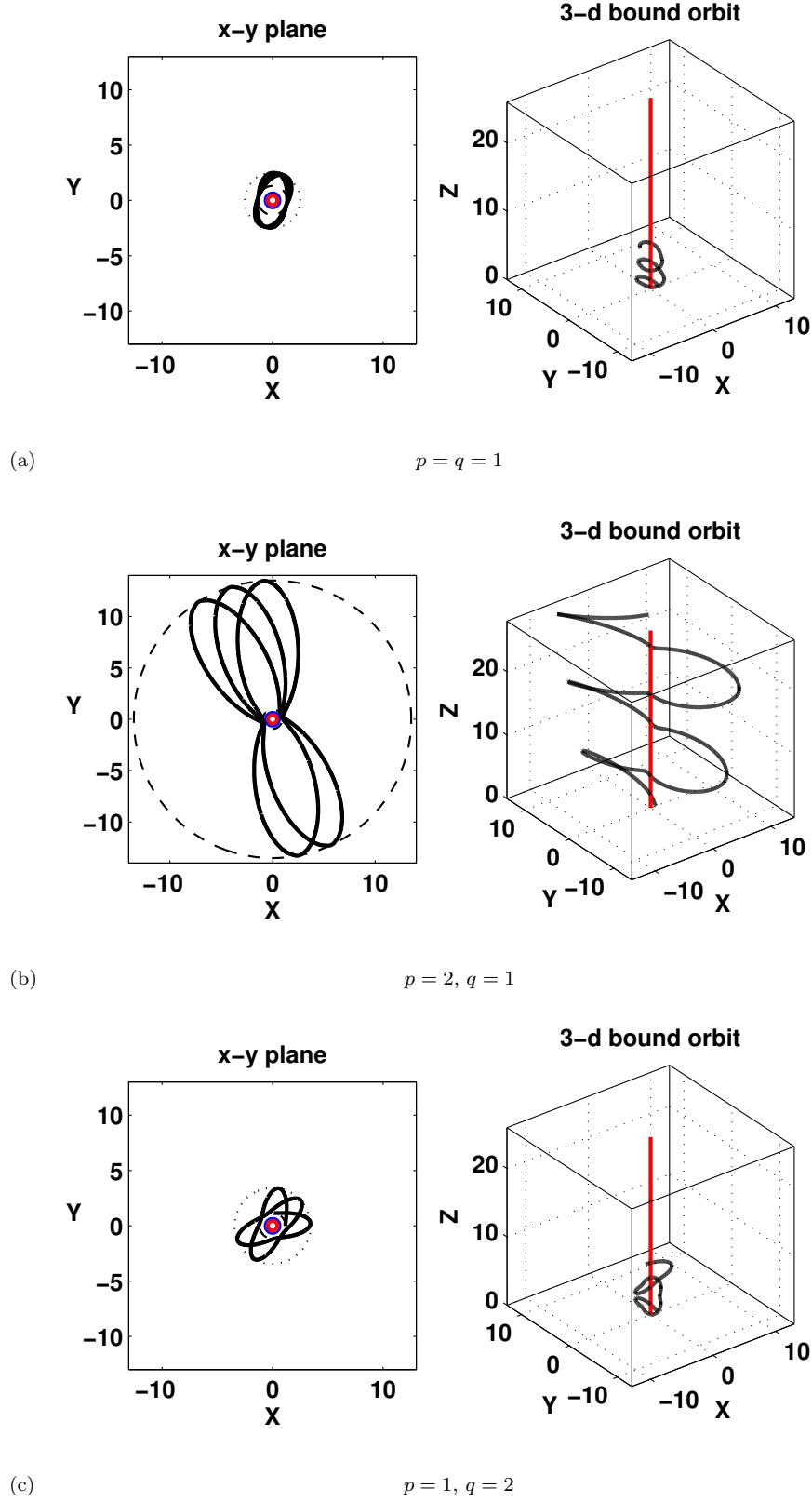


FIG. 10. The bound orbit of a massive test particle with $E = 0.9931$, $L_z = 0.01$ and $p_z = 0.015$ in the space-time of a (p,q) -string with $\gamma = 0.2$, $\beta_1 = 8$, $\beta_2 = 0.5$, $\beta_3 = 0.99$ and different choices of $(p,q) \equiv (n,m)$. The dotted circles denote the minimal and the maximal radius of the bound orbit, while the blue and the red circles indicate the radius of the gauge and scalar field cores, respectively.

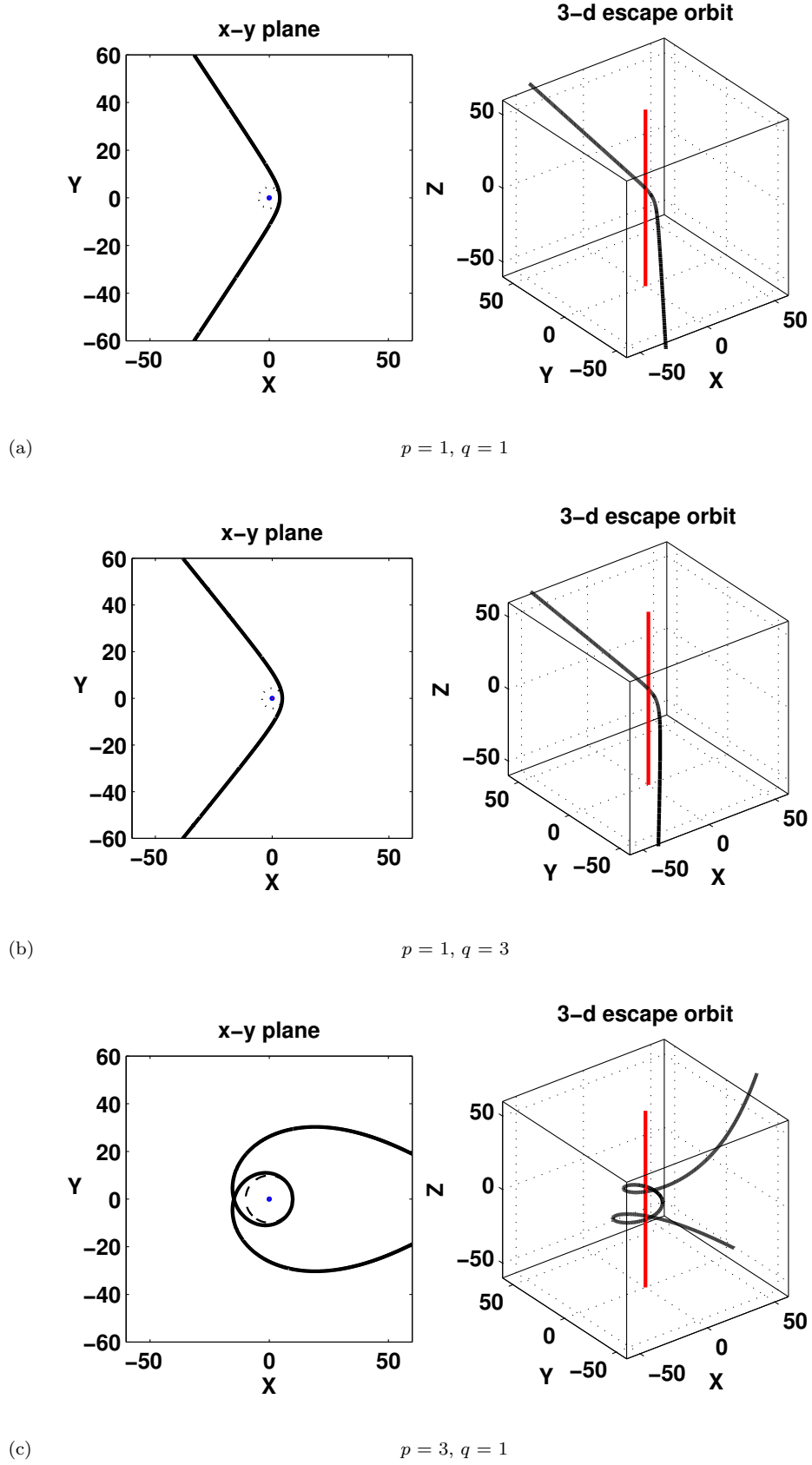


FIG. 11. The escape orbit of a massless test particle with $L_z = 0.2236$, $E = 0.08$ and $p_z = 0.05$ in the space-time of a (p,q) -string with $\gamma = 0.2$, $\beta_1 = 8$, $\beta_2 = 0.5$, $\beta_3 = 0.99$ and different choices of $(p,q) \equiv (n,m)$. The blue dot denotes the core of the string, while the dotted line denotes the circle with minimal radius of the orbit, i.e. closest approach of the particle to the string.

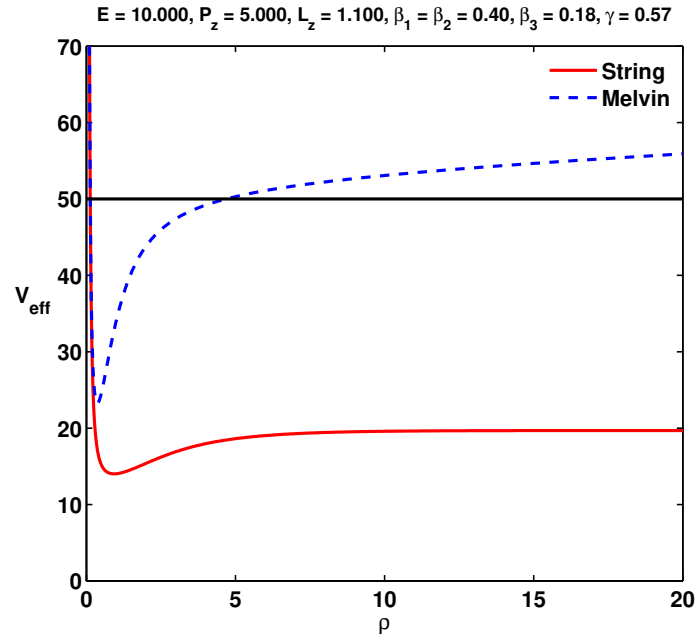


FIG. 12. The effective potential $V_{\text{eff}}(\rho)$ is shown for a Melvin solution (dashed) and in comparison for a string solution (solid) for $E = 10$, $p_z = 5$, $L_z = 1.1$ and coupling constants $\beta_1 = \beta_2 = 0.4$, $\beta_3 = 0.18$ and $\gamma = 0.57$. The horizontal solid line denotes the value of \mathcal{E} .

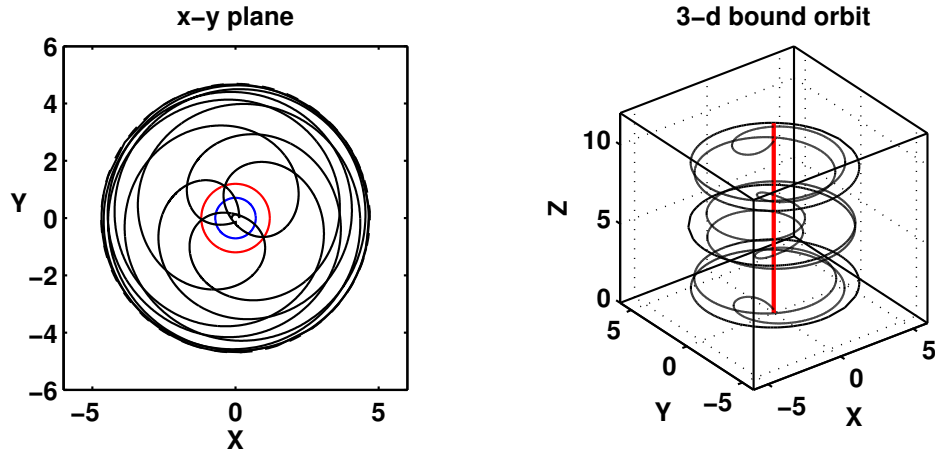


FIG. 13. The bound orbit of a massless test particle with $E = 10$, $L_z = 1.1$, $p_z = 5$ moving in a Melvin space-time with $\beta_1 = \beta_2 = 0.4$, $\beta_3 = 0.18$, $\gamma = 0.57$. The blue and the red circle indicates the radius of the gauge and scalar field cores, respectively.

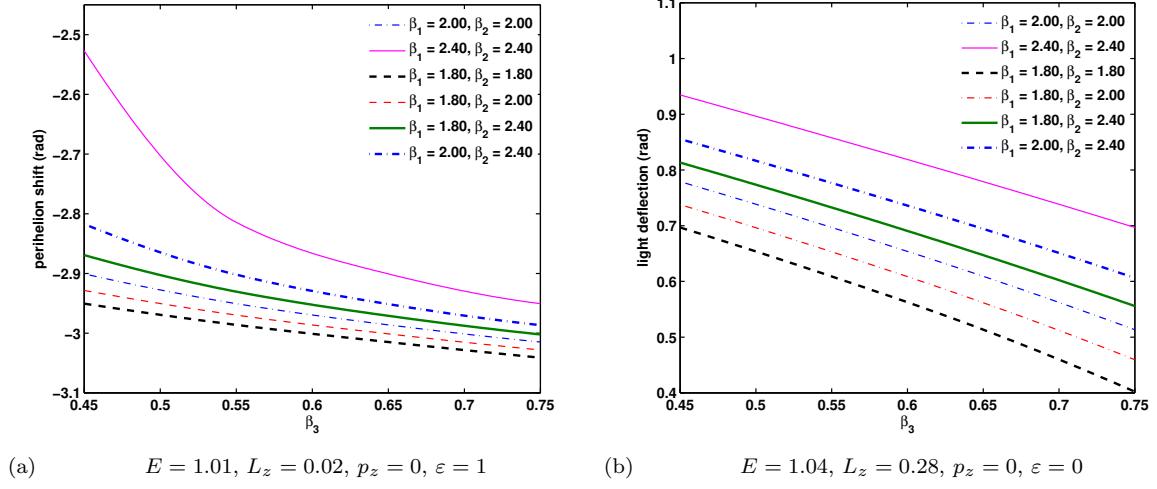


FIG. 14. The dependence of the perihelion shift of a planar bound orbit of a massive test particle with $E = 1.01$, $L_z = 0.02$ on β_3 and (left) and the dependence of the deflection angle of a planar escape orbit of a massless test particle with $E = 1.04$, $L_z = 0.28$ on β_3 (right).